THERMODYNAMIC CHARACTERIZATION OF SOLIDIFICATION AND DEFECTS THAT OCCUR IN Mg-ALLOY AM60

M. Vončina [*], M. Petrič, P. Mrvar, J. Medved

University of Ljubljana, Faculty of Natural Science and Engineering, Department of Materials and Metallurgy, Ljubljana, Slovenia

Abstract

The AM60 alloy was thermodynamically examined using chemical analysis, thermodynamic calculation made by ThermoCalc program, "in situ" thermal analysis and differential scanning calorimetry (DSC), whereas the microstructure constituents were confirmed using optical and scanning electron microscopy (SEM).

At the eutectic temperature of 437 °C the equilibrium solubility of Al in Mg is 12.6 wt. % Al. On the boundaries of the primary Mg grains the intermetallic compound of $Al_{12}Mg_{17}$ is precipitating according to the solvus line of the Mg-Al phase diagram. Solidification of the AM60 alloy has been investigated using "in situ" simple thermal analysis. The investigation of solidification has been taking place by evaluation of the cooling curves in connection with metallographic examinations, differential scanning calorimetry and thermodynamic calculations. All defects, nonmetallic inclusions and intermetallic compounds that occur in investigated AM60 alloy were identified.

Keywords: AM60 Mg-alloy; Thermodynamic calculation; Inclusions; Differential scanning calorimetry (DSC).

1. Introduction

Aluminium and magnesium are two most important lightweight metals used in automotive applications. The increasing need to lower the fuel economy has created a huge interest in the development of lightweight automotive structures, for aircraft parts, car parts, etc. Magnesium alloy products are 34 % lighter than aluminium and 76 % lighter than steels and show high light-to-weight ratio (UTS=36 KSI / 243 MPa). They show good corrosion resistance and good mechanical properties. The disadvantages of Mg processing occur due to technological melting processes, casting and working of the magnesium alloys, whereas all Mg alloy components-painted or unpainted-are fully recyclable. Therefore, fully understanding of solidification and cooling are needed for the optimization of the technological processes. Basic magnesium alloys Mg-Al (marked by ASTM as AMxy) contain from 2 to 9 wt. % Al [1-3].

The majority of magnesium elements is produced by means of sand or die casting. Despite Mg-based alloys are claimed to exhibit good casting properties, they are dramatically difficult to cast properly [4].

Beside the casting technology one of the important problems, which are connected with recycling and also re-melting, is the presence of nonmetallic inclusions as well as non-homogeneous and unbalanced chemical composition in ingots of magnesium alloys. The latter has influence on a portion of inter-metallic compounds such as $Mg_{17}Al_{12}$ and Al_4Mn. It has been found, that different input materials with chemical composition within valid standards have consequences on different technological, thermal, physical and mechanical properties. As demonstrated some authors [5] the microstructure of Mg-alloys for high pressure die casting process (HPDC) is a strong function of Al concentration such that alloys with 4–6 wt. % Al typically result in a well-defined skin region, related to the formation of the so-called externally solidified crystals (ESCs). Microstructure is also affected by local cooling rates that depend on the detailed structure of the casting and in particular local wall thickness. Shrinkage pores and gas pores are both observed in AM60 [6-8].

The most conventional way of melt purification is adding fluxes to the melt during melting, which contains chloride salts [9, 10] and/or fluoride salts [11]. It is true that some commercial fluxes can effectively remove nonmetallic inclusions from the melt of magnesium alloys, but the effects of these flux additions on decreasing the impurity elements of magnesium melt are not very satisfactory [12]. What is more, using fluxes may result in loss of alloying elements from the melt and secondary pollution through bringing in some nonmetallic impurity elements like F and Cl.

[*]*Corresponding author: maja.voncina@omm.ntf.uni-lj.si*

2. Experimental

For purpose of thermodynamic characterization of solidification and determination of defects, nonmetallic inclusions and intermetallic compounds, that occur in investigated AM60 alloy, following investigation methods were done on different AM60 alloys (from various manufacturers) in the high pressure die cast and gravity cast (blocks) state: chemical analysis, thermodynamic calculation, which was made by ThermoCalc program, "in situ" thermal analysis, differential scanning calorimetry (DSC), optical and scanning electron microscopy (SEM).

The "in situ" thermal analysis were made in the laboratory. The measuring process started with casting of the investigated molten metal into the sand measuring cell. Cooling curves were plotted and the characteristic solidification temperatures were marked. Furthermore, the chemical analysis was made and the specimens for DSC and optical and SEM were prepared out of castings from "in situ" thermal analysis. DSC was made on Jupiter 449c Instrument (NETZSCH) in order to determine the influence of defects and various inclusions on the solidification characteristics. To analyze the microstructure components optic microscope OLYMPUS BX61 equipped with video camera DP70 and analySIS 5.0 program was used and to identify the defects, nonmetallic inclusions and inter-metallic compounds that occur in investigated AM60 alloy, SEM JEOL 5610 with EDS and electron microanalyzer JEOL SUPERPROBE 733 with two WDS spectrometers was used.

3. Results and disscusion
3.1 Thermodynamic calculation

Thermodynamic calculations (Fig.1 and 2) were made by the ThermoCalc software TCW5 using SSOL database according to the chemical composition given in Table 1. Furthermore, all the equilibrium phases and their temperature range of stability were calculated for all four investigated samples from AM60 alloy (Fig.1). Fig.1 shows that the first phase to appear is the primary crystals of α_{Mg} from 616 to 639 °C and start growing. During the cooling the solubility of the alloying elements in α_{Mg} changes, which is shown with the shading. The intermetallic compounds Al_8Mn_5 and Mg_2Si also precipitates between liquidus and solidus temperature. The intermetallic compound $Al_{13}Fe_4$ forms from 515 to 548 °C, respectively, but the portion of it is very low. The intermetallic compound AlMnSi-β forms from 504 to 530 °C, respectively. At approximately 285 °C the intermetallic compound AlMn forms at the equilibrium conditions. It can be concluded that regarding the small changes in the chemical composition of AM60 alloy, although all are in the range of standard, the transformation temperatures of various phases, can significantly change.
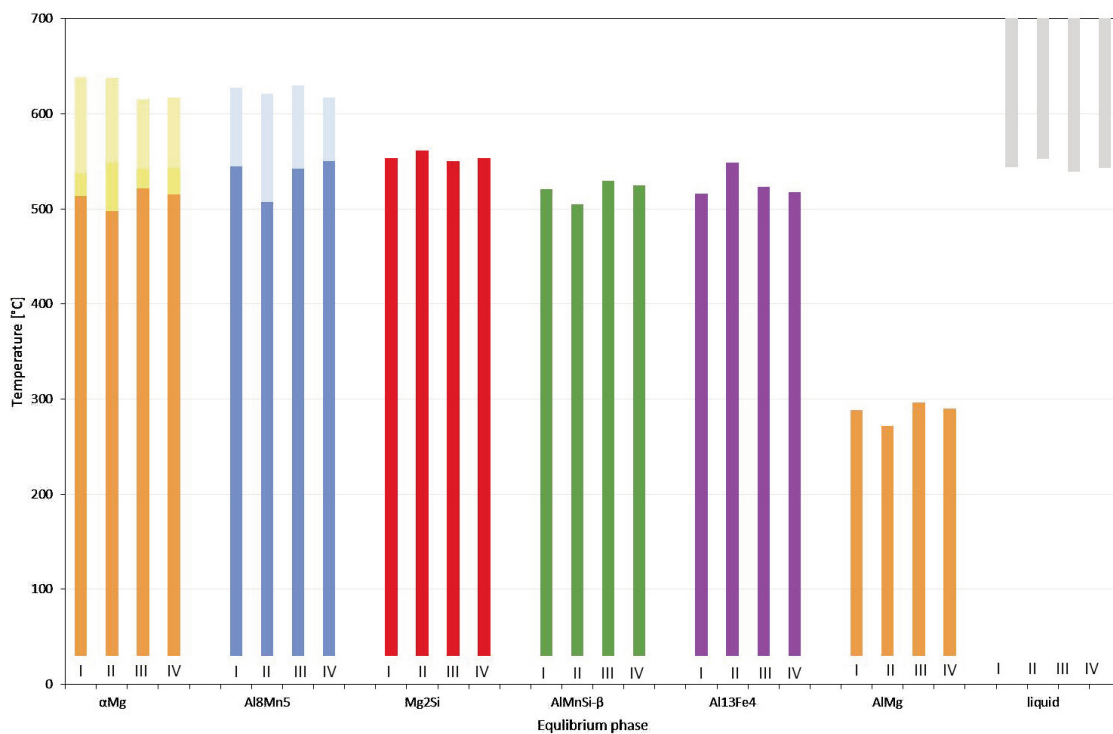
Figure 1. *Histogram of phase equilibriums in various AM60 alloys.*
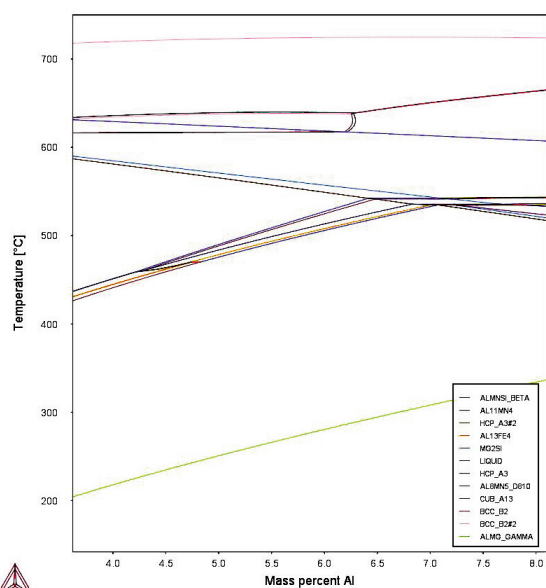
Figure 2. *Isopleth phase diagram Mg – Al – Mn at 0.3056 wt. % Mn, 0.0294 wt. % Si and 0.0032 wt. % Fe.*

Table 1. *Chemical composition according to the standard EN 1753 and of investigated samples from AM60 alloy/ wt.%.*

Element	AM60	I	II	III	IV
Al	5.8−6.40	6.28	5.84	6.33	6.43
Zn	<0.20	0.1267	0.056	0.075	0.087
Mn	>0.3	0.3056	0.355	0.34	0.359
Cu	<0.008	0.005	0.0037	0.0079	0.0054
Si	<0.05	0.0294	0.0369	0.0345	0.0364
Fe	<0.004	0.0032	0.003	0.003	0.003
Ni	<0.001	<0.0008	<0.0008	<0.0008	<0.0008
Mg	remain	remain	remain	remain	remain

3.2 "In situ" simple thermal analysis and solidification process

An "In situ" simple thermal analysis is an investigation and controlling method which is used in order to follow the solidification and cooling processes of the alloys. In this way the microstructure and properties can be determined indirectly [13]. In this case, "In situ" simple thermal analysis was used to confirm the solidification characteristic predicted with simulation program ThermoCalc.

Fig.3 shows the cooling curves end the corresponding microstructure. The liquidus (T_L), solidus (T_s) temperature and the temperature of the eutectic crystallization (T_E) were determined from cooling curves of DSC. Measured cooling rate was approximately 5 K/s. Liquidus temperature is at 607.6 °C. Next change on the cooling curves was detected at 509.4 °C what corresponds to nonequilibrium eutectic crystallization. Simple thermal analysis of the Mg-Al alloys shows that another eutectic crystallization appears at 432.9 °C at all investigated alloys.

Eutectic (α_{Mg} + $Al_{12}Mg_{17}$) forms along the boundaries of α_{Mg} crystal grains (Fig.3). Here the local increasing in fraction of aluminium in the melt occurs due to the aluminium segregation and therefore the nonequilibrium eutectic solidification takes place. The intermetallic compound Al_4Mn forms, whereas the part of aluminium in the melt reacts with manganese at lower temperature and it has decreasing effect of the aluminium fraction in the solid solution. At higher temperature this phase has a different stoichiometry, $Al_{11}Mn_4$ [1, 14].

Materials with very similar chemical composition can have different casting ability and technological properties as well as mechanical properties. The reason for that is mostly in the quantitative portion of inter-metallic compounds, inclusions, etc. [7].
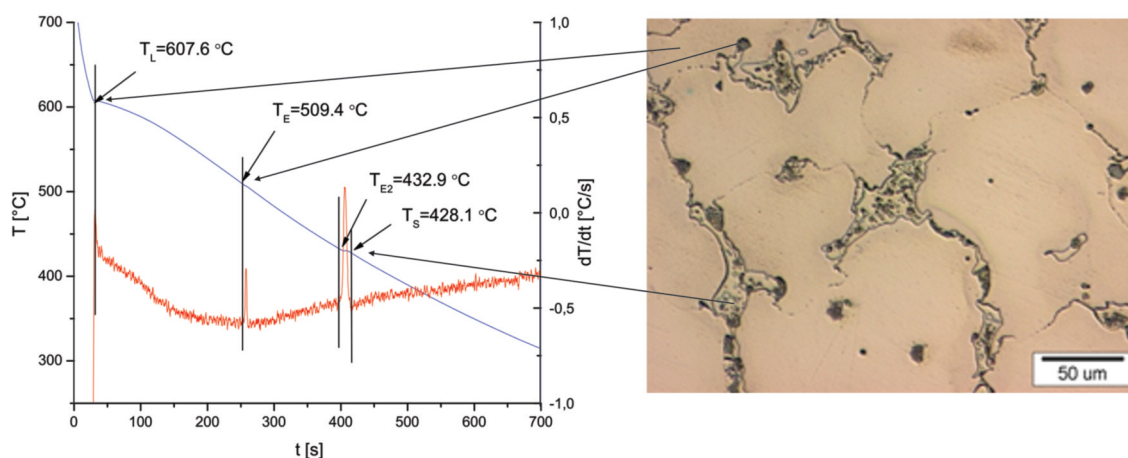
Figure 3. *Cooling curve and microstructure of AM60 alloy at cooling rate 5.7 K/s*

3.3 Simultaneous thermal analysis

Using the apparatus for DSC, the AM60 alloy was analyzed. The results are presented in the form of heating and cooling curves (Fig.4). During the heating process, the melting starts at solidus temperature (T_S), which is detected at 553.6 °C. The liquidus temperature is at (T_L = 605.5 °C). From DSC the liquidus temperature could be determined from cooling curve at 610.4 °C. Another reaction was detected at 505.7 °C, which corresponds to the solidification of $Al_{11}Mn_4$ phase. Because the local micro segregation happened during the relatively slow solidification process (cooling rate = 10 K/min) in the last solidified areas which are rich in Al, the eutectic reaction occurred ($L \rightarrow \alpha_{Mg} + Al_{12}Mg_{17}$) at 430.9 °C.

From to the microstructure of alloy AM60 alloy presented in Fig.5 the following micro constituents could be seen: primary crystals α_{Mg}, intermetallic compounds $Al_{12}Mg_{17}$ and Al_4Mn. All alleged micro constituents are in accordance with the chemical composition of alloy and the calculated equilibrium phase diagram (Fig.2).

When different specimens from different input materials (of various manufacturers) were tested the deviations occurred, whereas the liquidus and eutectic temperature varied (Fig.6). The solidification enthalpy also varied, which could be assigned to the impurities and inclusion in investigated alloy. The higher is solidification enthalpy, less inclusions and impurities is in the alloy. From this reason, all
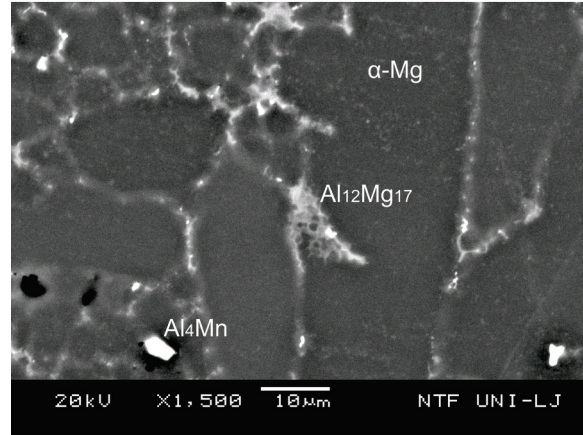
Figure 5. *Microstructure of AM60 alloy.*
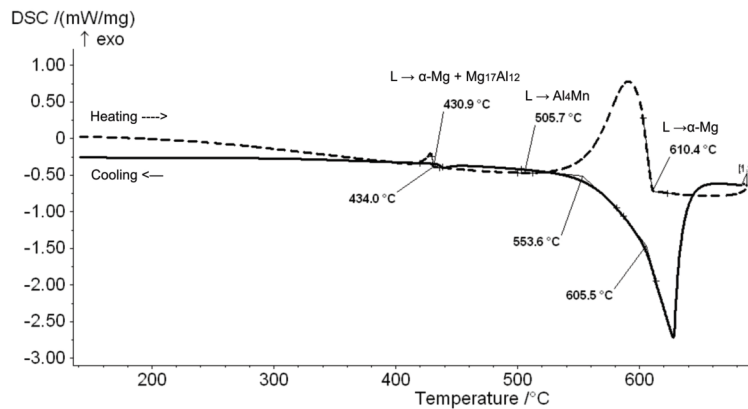
Figure 4. *Heating and cooling DSC curve of the AM60 alloy.*
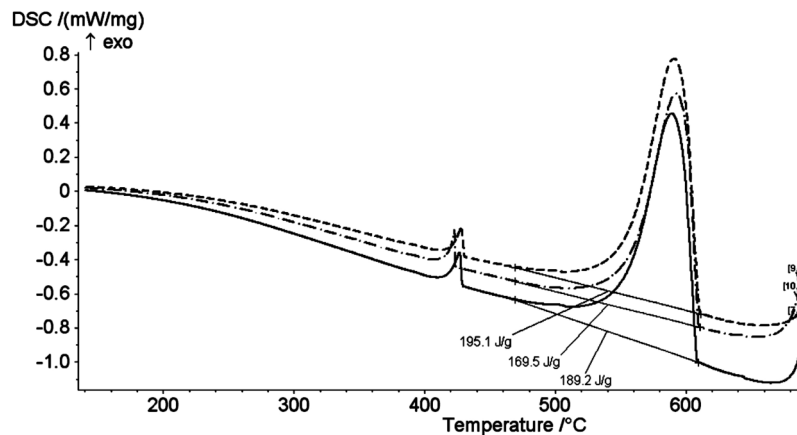
Figure 6. *DSC cooling curves of AM60 alloys from different manufacturers: alloy I (hole line), alloy II (dot-stripe line) and alloy III (stripped line).*

detected defects, nonmetallic inclusions and intermetallic compounds that occurred in investigated AM60 alloy were analyzed.

3.4 Defects, nonmetallic inclusions and inter-metallic compounds

In casting alloys nonmetallic inclusions appear. A part of these inclusions comes into the melt with recycling material and primary or secondary raw materials (oxidized surfaces, inclusions in alloy), and a part of them originates in the melt during re-melting process. In the investigated samples oxide, chloride and sulphide inclusions were identified. In Fig. from 7 to 13 the most frequent inclusions are presented: SiO_2 (Fig.7), $Al_xMn_yMg_zO_w$ (Fig.8), $\sim Ca_xMg_yMo_zO_w$
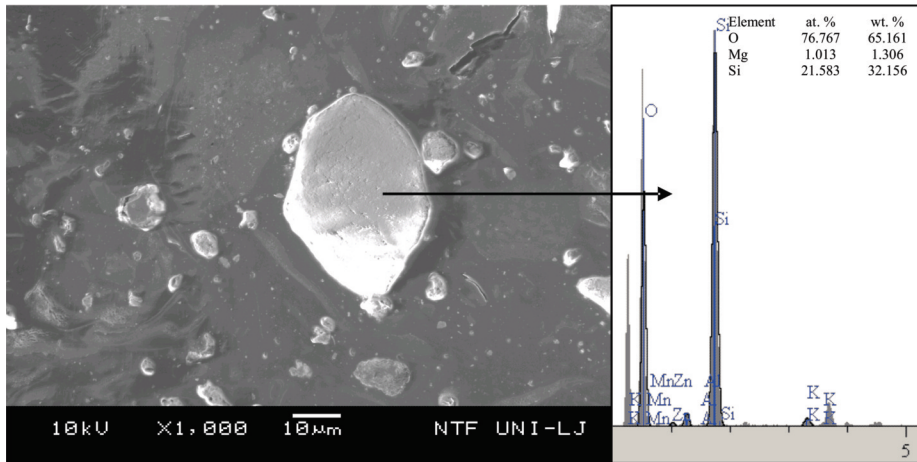
Figure 7. SEM micro photo of SiO_2 particle in AM60 alloy

Element	at. %	wt. %
O	76.767	65.161
Mg	1.013	1.306
Si	21.583	32.156
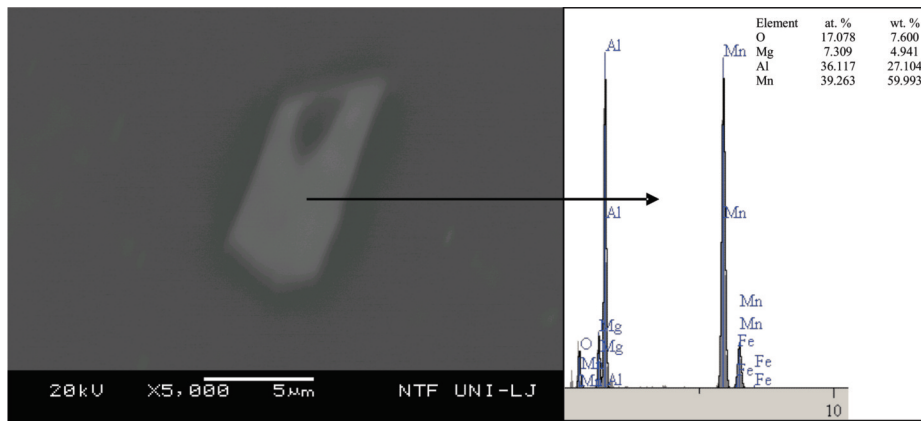
Figure 8. SEM micro photo of inclusion on base of oxygen, manganese, aluminium and magnesium

Element	at. %	wt. %
O	17.078	7.600
Mg	7.309	4.941
Al	36.117	27.104
Mn	39.263	59.993
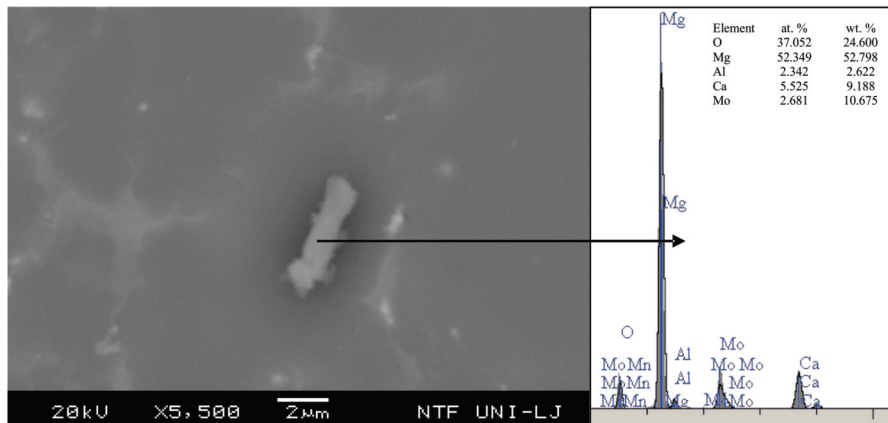
Figure 9. SEM micro photo of inclusion on base of molybdenum, calcium, magnesium and oxygen

Element	at. %	wt. %
O	37.052	24.600
Mg	52.349	52.798
Al	2.342	2.622
Ca	5.525	9.188
Mo	2.681	10.675

(Fig.9, accuracy is questionable because of the size of the inclusion), S-inclusion and Al_4Mn (Fig.10), Ca-inclusion (Fig.11), Cl-inclusion (Fig.12), C-inclusion (Fig.13), etc. Each inclusion was analyzed with energy dispersion spectrometer (EDS). The results of these analyses are portion of the elements, given in atomic and weight %. On the basis of these data the

stability of possible compounds with the help of thermodynamic program Tapp 2.1 (Table 2) was calculated. Measure for stability is the value of Gibbs energy (ΔG). The lower the value of ΔG is, the more stable the compound is. Singular calculations are made in dependence on temperature. The reference temperature is 600 °C, in most cases [13, 15].
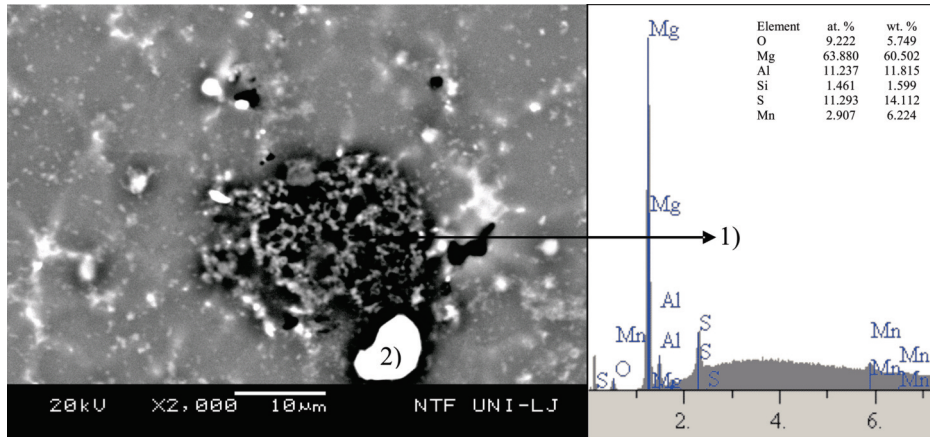
Figure 10. *SEM micro photo of complex inclusion: sulphide inclusion (1), inter-metallic compound Al$_4$Mn (2)*
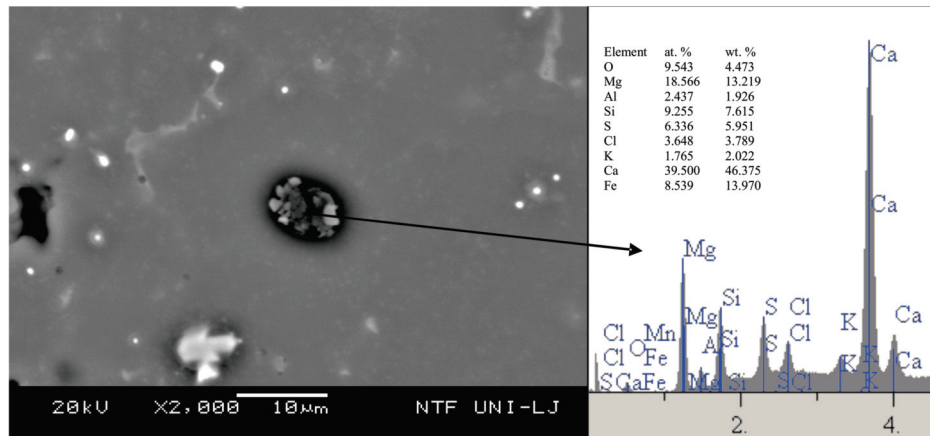
Figure 11. *SEM micro photo of inclusion on base of calcium.*
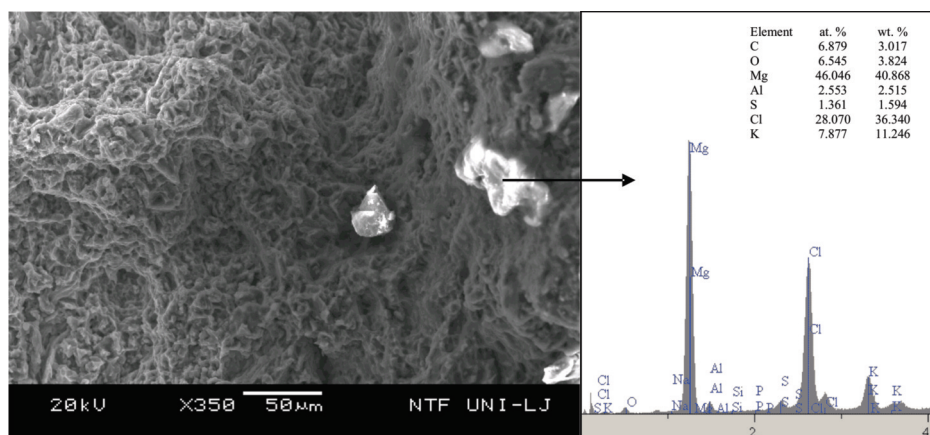
Figure 12. *SEM micro photo of inclusion on base of chlorine, fracture area.*
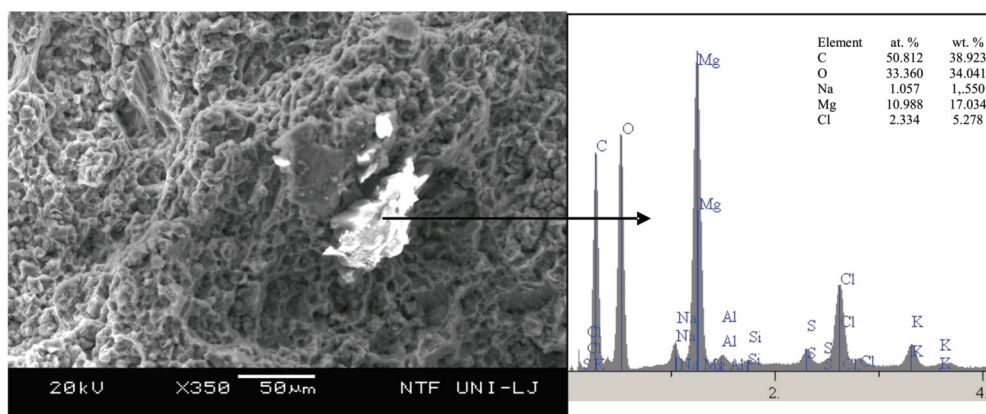
Figure 13. *SEM micro photo of inclusion on base of carbon.*

Table 2. *Stoichiometric compositions of inclusions and Gibbs energies (DG) (calculated by Tapp software)*

No.	Compound	Temperature of degradation (°C)	ΔG (kJ/mol)
1	$2MgO \cdot 2Al_2O_3 \cdot 5SiO_2$	600	-9389
2	$3CaO \cdot Al_2O_3 \cdot 3SiO_2$	600	-6985
3	$3CaO \cdot MgO \cdot 3SiO_2$	600	-4644
4	$K_2O \cdot 4SiO_2$	592	-4661
5	$CaO \cdot Al_2O_3 \cdot 2SiO_2$	600	-4488
6	$2CaO \cdot Al_2O_3 \cdot SiO_2$	600	-4253
7	$2CaO \cdot MgO \cdot 2SiO_2$	27	-3940
8	$CaO \cdot Al_2O_3 \cdot SiO_2$	600	-3478
9	$CaO \cdot MgO \cdot 2SiO_2$	600	-3249
10	$MgO \cdot Al_2O_3$	600	-2422
11	$2CaO \cdot SiO_2$	600	-2370
12	$2MgO \cdot SiO_2$	600	-2311
13	$CaO \cdot MgO \cdot SiO2$	27	-2296
14	$2CaO \cdot Fe_2O_3$	27	-2196
15	$MnO \cdot Al_2O_3$	27	-2183
16	Al_2O_3	600	-1756
17	$MgO \cdot SiO_2$	600	-1643
18	$MgO \cdot MoO_3$	600	-1592
19	$CaO \cdot MoO_3$	27	-1579
20	$CaO \cdot MgO$	600	-1336
21	$MgCO_3$	540	-1177
22	SiO_2	600	-967
23	$CaCl_2$	600	-915
24	MoO_3	600	-844
25	$MgCl_2$	600	-748
26	MgO	600	-674
27	CaO	600	-653
28	MoO_2	600	-653
29	CaS	600	-541
30	KCl	600	-529
31	$NaCl$	600	-495
32	$FeCl$	600	-474
33	MgS	600	-407
34	SiS_2	600	-312

4. Conclusions

From the cooling curves, the course of the solidification of the AM60 Mg-alloy was observed. Results from the "In situ" simple thermal analysis show the accordance of the solidification course with the equilibrium prediction of the solidification. Due to the presence of manganese in AM60 alloy the formation of the intermetallic compound Al_8Mn_5 takes place with decreasing concentration of the dissolved aluminium in the molten metal, but the formation of eutectic $(\alpha_{Mg} + Al_{12}Mg_{17})$ occurs at low cooling rate.

In casting alloys nonmetallic inclusions appear. A part of these inclusions comes into the melt with recycling material and primary or secondary raw materials (oxidized surfaces, inclusions in alloy), and a part of them originates in the melt during re-melting process. From quantitatively determined heat effect (solidification enthalpy) and from the characteristic points on "in situ" recorded cooling curves, it is possible to estimate the quality ratio of materials according to purity (portion of inclusions). In the investigated samples oxide, chloride and sulphide inclusions were identified.

References

[1] J. Medved, P. Mrvar, Materials Science Forum, 508 (2006) 603-608.

[2] K.U. Kainer, Magnesium Alloys and Technology. Weinheim: WILLEY – VCH, 2003, p. 254-272.

[3] H.A. Dorsam, Magnesium melting/casting and remelting in foundries. EFM Magnesium Seminar, Aalen, 2000

[4] B. Dybowski, A. Kielbus, Materials Science Forum, 782 (2014) 398-403.

[5] K. Vanna Yang, M.A. Easton, C.H. Caceres, Mater. Sci. Eng. A, 580 (2013) 191–195.

[6] S.G. Lee, A.M. Gokhale, Scr. Mater., 55 (4) (2006) 387–390.

[7] J. López, F. Faura, J. Hernández, P. Gómez, J. Manuf. Sci. Eng., 125 (3) (2003) 529-537.

[8]	Z. Yang, A. Maurey, J. Kang, D.S. Wilkinson, Materials Characterization, 114 (2016) 254–262.

[9]	W. Wang, G.H. Wu, Q.D. Wang, Y.G. Huang, M. Sun, W.J. Ding, Trans. Nonferrous Met. Soc. China, 18 (S1) (2008) 292–298.

[10]	G.H. Wu, W. Wang, M. Sun, Q.D. Wang, W.J. Ding, Trans. Nonferrous Met. Soc. China, 20 (2010) 1177–1183.

[11]	W. Jie, J.X. Zhou, W.H. Tong, Y.S. Yang, Trans. Nonferrous Met. Soc. China, 20 (2010) 1235–1239.

[12]	O. Lunder, T.K. Aune, K. Nisancioglu, Corros. Sci, 43 (1987) 291–295

[13]	P. Mrvar, J. Medved, M. Trbižan, A. Papež, J. Ramovš, Nekovinski vključki in intermetalne spojine v zlitini AM60, Zbornik referatov na 44. livarskem posvetovanju v Portorožu 2004.

[14]	P. Mrvar, M. Terčelj, G. Kugler, M. Fazarinc, J. Medved, RMZ - Materials and Geoenvironment, 53(2)(2006) 175-192.

[15]	P. Mrvar, J. Medved, M. Trbižan, A. Papež, J. Ramovš, Livar. vestn. 52 (2004) 146-159.